

## Electronic states in the stage-3 mercury chloride graphite intercalation compound

D. Marchesan, T. R. Chien, G. Wang, P. K. Ummat, and W. R. Datars

*Department of Physics and Astronomy, McMaster University, Hamilton, Ontario, Canada L8S 4M1*

(Received 2 November 1994; revised manuscript received 30 May 1995)

The electronic states of the stage-3 mercury chloride graphite intercalation compound ( $\text{HgCl}_2\text{-GIC}$ ) were investigated by the de Haas-van Alphen (dHvA) effect in the temperature range from 1.4 to 4.2 K with magnetic fields from 3 to 5 T. Three prominent dHvA frequencies,  $f_1=142.6$  T,  $f_2=533$  T, and  $f_3=788$  T are identified with the three modified graphite  $\pi$  bands expected for a stage-3 GIC. The cyclotron electron masses for the graphitic bands are measured, yielding  $m_1^*=0.09m_0$ ,  $m_2^*=0.17m_0$ , and  $m_3^*=0.19m_0$ . In addition, there is a low-frequency oscillation at  $f_0=82.5$  T with  $m_0^*=0.15m_0$ . The determination of the fractional charge distribution along the  $k_z$  direction of the three graphite layers of the stage-3 compound indicates that there is a deficiency of charge in the internal graphite layer relative to the layers adjacent to the intercalant. The charge fraction on the internal graphite layer is determined to be 0.25. The low-frequency  $f_0$  may result from the effect of an incommensurate superlattice, which forms a magnetic interferometer orbit.

### I. INTRODUCTION

Graphite intercalation compounds (GIC's) are formed by incorporating a layer of guest atoms or molecules, the intercalant, between layers of the graphite host. These compounds exhibit a unique staging phenomenon in which a constant number of graphite layers are separated by an intercalant layer, and a stage- $n$  GIC is composed of a series of  $n$  graphite layers separated by single intercalant layers. The GIC is a highly anisotropic layered structure possessing strong intraplanar binding forces relative to weak interplanar binding. These compounds provide a vehicle for studying a quasi-two-dimensional system.

Metal chloride graphite intercalation compounds constitute an important group of acceptor-type compounds.<sup>1</sup> However, the intercalation of these compounds only takes place in the presence of chlorine.<sup>2</sup> This makes high staging fidelity of samples difficult to obtain in the conventional two-zone oven method, due to its dependence on not only the temperature of the graphite and the metal chloride, but also the pressure of chlorine. Therefore, not many physical, structural, and electrical properties of the compounds have been investigated.

The conditions for intercalating large pieces of highly oriented pyrolytic graphite with  $\text{HgCl}_2$  were reported<sup>3</sup> and a pure stage-3  $\text{HgCl}_2\text{-GIC}$  was obtained with the sample in chlorine gas at a pressure of 800 mbar. Due to its high staging fidelity,  $\text{HgCl}_2\text{-GIC}$  was chosen for the investigation of the electronic properties of the acceptor-type GIC by the de Haas-van Alphen (dHvA) technique.

This work presents the results of the investigation of the electronic bands and charge distribution of the stage-3 acceptor  $\text{HgCl}_2\text{-GIC}$  by the dHvA effect. Measurements of the dHvA effect yield extremal cross-sectional Fermi areas which are perpendicular to the magnetic-field direction. Rotation of the sample, with respect to the field direction, allows a mapping of the Fermi surface. The experimental data related to the band structure are

interpreted with the Blinowski-Rigaux theoretical band-structure model.<sup>4</sup> The charge distribution along the  $c$  axis is derived from the observed dHvA frequencies. The possible effects of an incommensurate superlattice are also considered.

### II. EXPERIMENT

The starting material was highly oriented pyrolytic graphite (HOPG). Slabs of HOPG were cut into pieces of about  $2.5 \times 3.5$  mm<sup>2</sup> and the pieces were cleaved to a thickness of about 0.7 mm. The outer layer was removed by peeling. The pieces were then washed in an ultrasonic cleaner. Cleaned HOPG pieces were put into a glass container and dried under vacuum at an elevated temperature.

The stage-3  $\text{HgCl}_2\text{-GIC}$  was made using the method of Datars and Ummat. The HOPG and  $\text{HgCl}_2$  were placed in a sealed reaction tube and heated to a temperature of 250 °C with the graphite and intercalant at the same temperature. At this temperature,  $\text{HgCl}_2$  was a clear liquid and the pressure of  $\text{Cl}_2$  in the tube was 800 mbar. An intercalation time of 432 h (18 days) was required to form a fully developed, stage-3  $\text{HgCl}_2\text{-GIC}$  with a composition of  $\text{C}_{17.4}\text{HgCl}_2$  determined by the change in weight during intercalation. After the intercalation reaction was completed, each sample was washed with dilute HCl, deionized water, and acetone, and then dried. The  $\text{HgCl}_2\text{-GIC}$  is stable in air.

The stage index of the samples was determined with x-ray-diffraction measurements by using a powder diffractometer with  $\text{CuK}\alpha$  radiation. The x-ray diffraction spectrum is shown in Fig. 1. The spectrum reveals a pure staged sample with no diffraction peaks from mixed stages. A straight line was fitted to the reflection order  $l$  versus  $1/d_l$  and the value of  $I_c$ , the  $c$  axis repeat distance, was calculated from the slope of the line. The

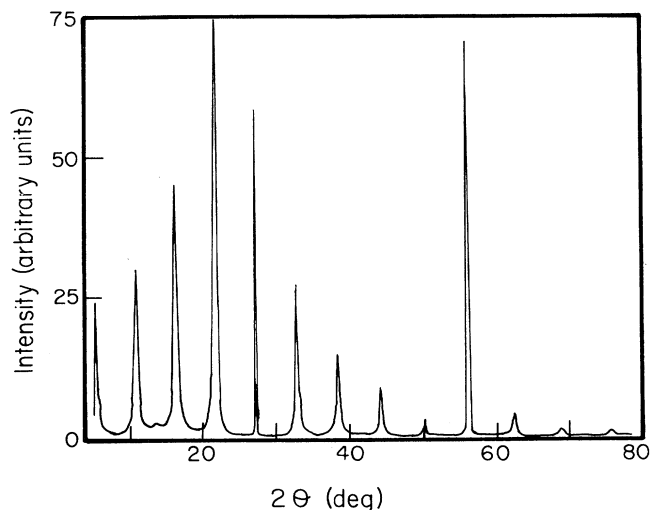


FIG. 1. (001) x-ray diffraction of the stage-3  $\text{HgCl}_2$ -GIC using  $\text{Cu } K\alpha$  radiation.

repeat distance of the stage-3  $\text{HgCl}_2$ -GIC was calculated to be 16.31 Å. This value of  $I_c$  is similar to that found previously for the stage-3 compound made from small natural flakes of carbon<sup>2</sup> and is the same as that obtained by Datars and Ummat.

The dHvA oscillations were observed with the low-frequency field modulation technique with a modulation frequency of either 47 or 517 Hz along the magnetic-field direction. Reproducible results were obtained from repeated experiments performed with four  $\text{HgCl}_2$ -GIC samples. The sample was put inside a set of coils, which consisted of a modulation coil, a rotatable pickup coil, and balance coil. The balancing coil was wound in an antiparallel fashion above the pickup coil in order to maximize the signal from the sample's oscillating magnetization. This set of coils was placed inside a 5.5-T superconducting solenoid. Both the dHvA frequency spectrum and the temperature dependence of the amplitude between 1.4 and 4.2 K were measured with the  $c$  axis of the sample parallel to the direction of the magnetic field.

### III. EXPERIMENTAL RESULTS

The dHvA oscillations shown in Fig. 2 consist of many frequencies as indicated by the complexity of the pattern. The frequencies are determined from the Fourier transform of the dHvA signal given in Fig. 3. The frequencies are 82.5, 142.6, 450.4, 533.0, 615.3, 705.0, and 788.0 T. The uncertainty of these values was determined from the results of the four samples to be  $\pm 0.3$  T. There is also a frequency of 330 T in Fig. 3. The oscillation with this frequency was the largest when a sample was cooled for the first time. It was smaller or not evident after subsequent cooling from room temperature. There is no explanation for this frequency at the present time.

The dependence of the frequencies of the dominant oscillations on the angle of the magnetic-field direction with

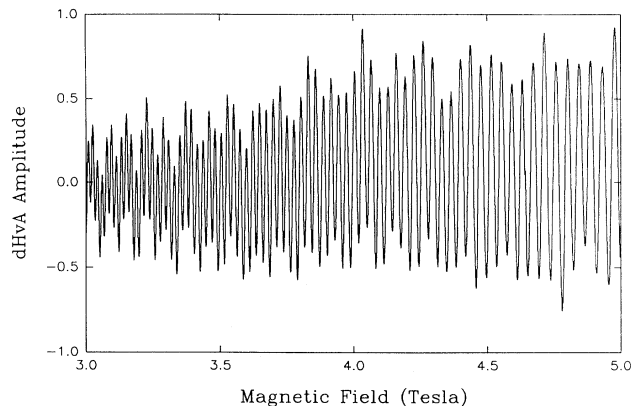


FIG. 2. dHvA oscillations of the stage-3  $\text{HgCl}_2$ -GIC observed at the second harmonic of the modulation field of 517 Hz for magnetic fields between 3 and 5 T. The temperature was 4.2 K and the dc field and modulation field were parallel to the  $c$  axis of the sample.

respect to the  $c$  axis was measured in the range  $0 < \Theta < 22^\circ$ . The oscillations with the  $c$  axis frequencies of 82.5, 142.6, 450.4, and 533 T followed a  $\sec\Theta$  dependence indicating that they are from cylindrical Fermi surface pieces directed along the  $c$  axis.

The carrier effective masses corresponding to the dominant frequencies were determined from the temperature dependence of the dHvA amplitude between 1.4 and 4.2 K. The dHvA amplitude is related to the sample temperature by the proportionality,<sup>5</sup>

$$A \propto \frac{T}{\sinh\left(\frac{bm^*T}{Bm_0}\right)}, \quad (1)$$

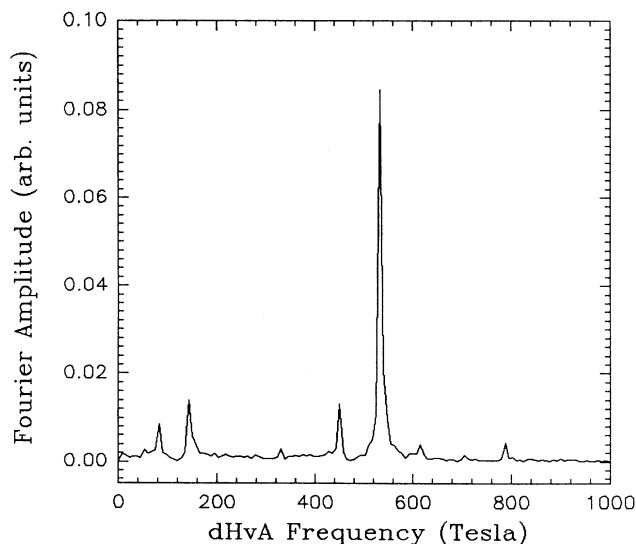


FIG. 3. Fourier transform of the dHvA oscillations for stage-3  $\text{HgCl}_2$ -GIC taken at 2.4 K.

where  $A$  is the dHvA amplitude at temperature  $T$  and magnetic field  $B$ ,  $m^*$ , and  $m_0$  are the cyclotron mass and free-electron mass, respectively, and  $b = 14.69 \text{ T K}^{-1}$ . The masses were determined for the oscillations with reasonably large amplitudes. The results are  $0.147m_0$  for the 82.5-T oscillation,  $0.086m_0$  for 142.6 T,  $0.0165m_0$  for 533 T, and  $0.190m_0$  for the 788-T oscillation.

#### IV. DISCUSSION

The assignment of the frequencies requires attention to the values of the frequencies, the cyclotron masses, and a comparison with the result from other chloride GIC's. Since the  $\text{HgCl}_2$  GIC is a stage-3 compound, three graphite energy bands are expected from the tight-binding calculation, due to the interaction between the three graphite layers. This interaction and the energy bands are expected to be similar in all the stage-3 chloride GIC's. The frequency 142.6 T is assigned to the first band, because it is similar to the first band frequencies of 152 and 172 T in the stage-3  $\text{SbCl}_5$  and  $\text{SbF}_6^-$  GIC's, respectively. The amplitude of the oscillation is also the larger of the two low frequencies. The frequency 533 T is assigned to the second band, because the oscillation with this frequency is dominant and then the ratio  $f_2/f_1$  is similar to those of the other two stage-3 GIC's. The assignment to third band is the most difficult. The frequency of 788 T is the closest to the third-band frequencies of the other stage-3 GIC's and is assigned to the third band. The cross-sectional Fermi areas are determined by the relation  $A_f = (4\pi^2 e/h)f$  yielding  $A_1 = 0.014 \text{ \AA}^{-2}$ ,  $A_2 = 0.051 \text{ \AA}^{-2}$ , and  $A_3 = 0.075 \text{ \AA}^{-2}$ . The other frequencies appear to be combinations with the lowest frequency 82.5 T, which is labeled  $f_0$ . The frequencies 450.4 and 615.3 T are within 0.2 T of  $f_2 - f_0$  and  $f_2 + f_0$ , respectively; the frequency 705 T is within 0.5 T of  $f_3 - f_0$ . Thus, there is agreement to within the experimental uncertainty.

The Blinowski-Rigaux band-structure model for stage-3 graphite acceptor compounds incorporates a simple tight-binding method and considers nearest carbon atom interactions. The stage-3 GIC is treated theoretically as a set of three equivalent, independent graphite layers limited by the intercalant layers. This model accounts for electrostatic effects, due to the accumulation of excess charge on the two graphite layers adjacent to the intercalant. Three valence bands are predicted for the stage-3 GIC, occurring from the interaction of the adjoining graphite layers. The electron dispersion is assumed to be independent of the intercalant and the number of electrons transferred from the graphite. There is no dispersion along the  $c$  axis in this model. The Fermi surface is predicted to be a straight cylinder along the  $c$  axis at each corner of the hexagonal Brillouin zone for each band with one dHvA frequency corresponding to each band. The angular dependence  $f(\theta)$  of the dHvA frequencies for angles  $\theta = 0^\circ - 22^\circ$ , where  $\theta$  is measured between the  $c$  axis and the main field direction, indicates that  $f(\theta) \propto \sec \theta$ , supporting the description of the Fermi surface as being a set of concentric straight cylinders.

The energies of the three valence bands are given by

$$E_1 = \delta - |X|, \quad (2)$$

$$E_2 = -[\delta^2 + \gamma_1^2 + |X|^2 - \sqrt{\gamma_1^4 + [(4\delta^2 + 2\gamma_1^2)|X|^2]^{1/2}}]^{1/2}, \quad (3)$$

$$E_3 = -[\delta^2 + \gamma_1^2 + |X|^2 + \sqrt{\gamma_1^4 + [(4\delta^2 + 2\gamma_1^2)|X|^2]^{1/2}}]^{1/2}, \quad (4)$$

where  $|X| = 3/2\gamma_0 b k$ ,  $k$  is the distance from  $\mathbf{k}$  to the  $U$  point, and  $b$  is the nearest-neighbor distance. The interaction energy between the nearest carbon atoms in the same plane is represented by  $\gamma_0$  and  $\gamma_1$  is the interaction energy between nearest carbon atoms in adjacent layers,  $\delta$  is proportional to the potential-energy difference between external and internal graphite layers. The Fermi area dependence on energy is differentiated to obtain the cyclotron mass.

The following values of the model parameters  $\gamma_0 = 2.9 \text{ eV}$ ,  $\gamma_1 = 0.31 \text{ eV}$ ,  $\delta = 0.12 \text{ eV}$  and  $E_F = -0.70 \text{ eV}$  yield the best agreement between the theoretically and experimentally determined Fermi areas. The parameters for pristine graphite are reported<sup>6</sup> as  $\gamma_0 = 3.16 \text{ eV}$  and  $\gamma_1 = 0.39 \text{ eV}$ . The energy-band structure near the  $U$  point is shown in Fig. 4.

The accuracy of the predictions of the model is reasonable. The largest discrepancy between the experimental and theoretical Fermi areas is approximately 7%, but the effective-mass values are in good agreement, as shown in Table I. The use of the Blinowski-Rigaux model provides an approximate framework for the analysis of the  $\text{HgCl}_2$ -GIC experimental results, yielding energy dispersion relations and charge-transfer values. The determination of the interrelated model parameters  $\gamma_0$ ,  $\gamma_1$ ,  $\delta$ , and  $E_F$  are not unique. Thus, the validity of the model and the model parameters used is justified on a self-consistency basis.

The charge distribution between the three adjoining graphite layers is determined by

$$2\delta = 0.1 \text{ eV} + f / (57.6z - 2.7) \text{ eV}, \quad (5)$$

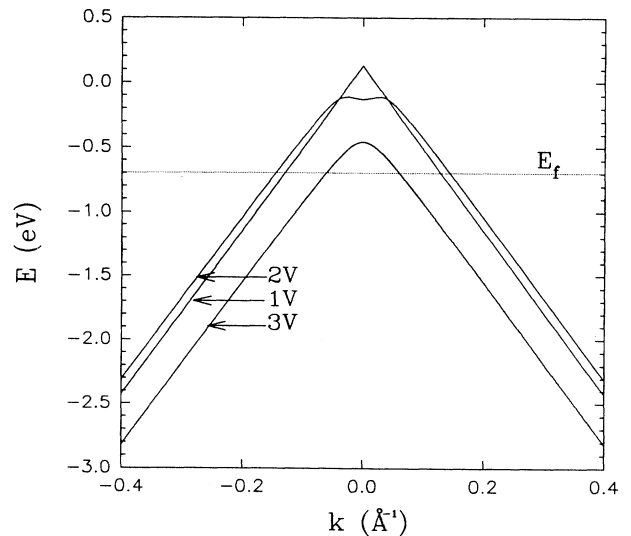


FIG. 4. The energy-band structure near the  $U$  point for the stage-3  $\text{HgCl}_2$ -GIC. The three valence bands are labeled as 1V, 2V, and 3V for the first, second, and third valence bands.

TABLE I. Experimental and calculated Data for the HgCl<sub>2</sub>-GIC.

Frequency (T)	Fermi experiment	Area (Å <sup>-2</sup> ) calculated	Effective experiment	Mass ( <i>m</i> / <i>m</i> <sub>0</sub> ) calculated
83	0.008		0.15	
143	0.014	0.013	0.09	0.09
533	0.051	0.055	0.17	0.16
788	0.075	0.070	0.19	0.19

where *z* is the fraction of charge on the center layer. The charge transfer per carbon atom *f*/*l* is given by

$$\frac{f}{l} = \frac{a^2\sqrt{3}}{4\pi^2n} \sum_{i=1}^3 A_{Fi}, \quad (6)$$

where *n* is the stage number, *a* is the length of the primitive translation vector, and *A<sub>Fi</sub>* is the extremal Fermi area of the *i*th band. With the choice of  $\delta=0.12$ , the charge transfer per carbon atom *f*/*l* is 0.012 yielding the fraction 0.25 of charge on the center graphite layer. The remaining fractional charge is distributed equally on the two outside graphite layers. The charge transfer per HgCl<sub>2</sub> molecule is 0.21. These results are similar to those derived by Markiewicz<sup>7</sup> for other stage-3 compounds for which the charge transfer per intercalant molecule was in the range 0.23–0.57 and the interior layer fraction was between 0.16 and 0.24.

Some interesting properties of the low-frequency oscillation at 82.5 T can be indicated although its microscopic origin is not known. This oscillation interacts to produce combination modes. The ratio of cyclotron mass to Fermi area for this oscillation is 18.6, which is significantly larger than the ratios 6.2, 3.2, and 2.5 for oscillations *f*<sub>1</sub>, *f*<sub>2</sub>, and *f*<sub>3</sub>, respectively. This indicates that the 82.5-T oscillation is different in nature from those assigned to the three graphitic bands.

We discuss now whether the magnetic interferometer effect<sup>8</sup> that was used to explain the low frequencies of the stage-1 and stage-2 AsF<sub>5</sub>-GIC's is present in the HgCl<sub>2</sub> GIC. In this effect, a folding of the warped cylindrical Fermi surface on itself by an intercalant superlattice provides two paths that interfere when there is a magnetic breakdown. This produces a low frequency and forms a set of sum and difference frequencies with the cylinder frequency. An intercalant ordering is required to facilitate the zone folding. X-ray-diffraction studies<sup>9</sup> of the HgCl<sub>2</sub> GIC show an oblique lattice and a domain structure, which are incommensurate with the graphite lattice. An incommensurate superlattice forms gaps in the electronic spectrum, which, in principle, are infinite in number. However, usually only the lowest gaps produce significant modulations that can modify the dHvA spectrum<sup>10</sup> and forms new frequencies that may disappear at high fields, due to a magnetic breakdown. In the hexagonal environment of graphite, the magnetic interferometer effect can produce seven frequencies; the interferometer frequency *f*<sub>0</sub> and the larger frequencies *f*, *f*+*f*<sub>0</sub>, . . . *f*+6*f*<sub>0</sub>. If we choose *f*=450.4 T and *f*<sub>0</sub>=82.5 T, the frequencies 533 and 615.3 T are in agreement with *f*+*f*<sub>0</sub> and *f*+2*f*<sub>0</sub>, but 705 and 788 T differ

by 6 to 7 T from *f*+3*f*<sub>0</sub> and *f*+4*f*<sub>0</sub>, respectively. Thus, there is only partial support for the interferometer effect in the HgCl<sub>2</sub> GIC. Also, it would have to be shown that the effect can be found in magnetization measurements that were taken in this experiment, since the classical calculation indicates that it should affect only transport measurements such as the resistivity. However, it can be considered an alternate explanation of the HgCl<sub>2</sub> GIC dHvA spectrum and provides an explanation of the low frequency as an interferometer orbit.

Another unusual feature of the data is that the dHvA oscillations were not observed when the magnetic field was tilted away from the *c* axis by more than 22°, since the dHvA effect from Fermi-surface cylinders should exist for larger angles. This indicates extra scattering at larger angles. This could come from the boundaries of the graphite layers or could be explained by another interesting mechanism resulting from the two-dimensional properties of the material.

The present results extend the understanding of the electronic properties of stage-3 GIC's. For the HgCl<sub>2</sub>-GIC, there are single frequencies at 142.6, 533, and 788 T from three bands, there is also a low frequency of 82.5 T with an unknown origin. The frequencies of the other stage-3 compounds that have been investigated by the dHvA effect can be classified in a similar manner by considering a group of closely spaced frequencies for each band. The reason for the splitting is not clear at this time and could be a result of sample inhomogeneity or a more fundamental cause. We interpret the previous work on stage-3 GIC's in the following way. For the stage-3 SbCl<sub>5</sub>, Takahashi, Iye, and Tanuma<sup>11</sup> found a low frequency of 62.5 T and frequencies of 127 and 149 T for band 1, 641 T for band 2, and 909 T for band 3. Then Wang *et al.*<sup>12</sup> observed a low frequency of 37 T and sets of frequencies 152–179 T, 620–665 T, and 782–840 T for the three bands.

For the stage-3 AsF<sub>5</sub> GIC, Iye, Takahashi, and Tanuma<sup>13</sup> observed a low frequency of 72.5 T and three groups at 100–109 T, 512–580 T, and 833–877 T that are attributed to the three bands. The frequencies observed by Markiewicz *et al.*<sup>14</sup> can be attributed to the first band (100 T) and the third band (900–1000 T).

The results for the stage-3 HNO<sub>3</sub>-GIC by Tanuma, Iye, Takahashi, and Koike<sup>15</sup> have low frequencies of 58, 83 T and frequencies of 167, 518, and 830 T for the three bands. Finally, Wang, Ummat, and Datars<sup>16</sup> reported frequencies of 172, 656, and 852 T for the three bands of the SbF<sub>5</sub>-GIC, but no low frequency was observed.

In certain cases there are also one or more frequencies in between 300 and 400 T that are not explained. For example one appeared after the first cool down at 330 T in the HgCl<sub>2</sub>-GIC, but disappeared gradually after subsequent temperature cycles. Thus, it appears that the dHvA effect for all the stage-3 GIC's can be interpreted in a similar way.

## V. CONCLUSIONS

The electronic properties of the stage-3 HgCl<sub>2</sub>-GIC were investigated by the dHvA effect. The three dom-

inant dHvA oscillations associated with the basic graphitic bands have been identified, possessing frequencies  $f_1=142.6$  T,  $f_2=533$  T, and  $f_3=788$  T. An additional oscillation at 82.5 T was observed. The effective-mass results are  $m_1^*=0.09m_0$ ,  $m_2^*=0.17m_0$ , and  $m_3^*=0.19m_0$ . The mass for the low-frequency oscillation is  $m_0^*=0.15m_0$ .

The experimental results for HgCl<sub>2</sub>-GIC were compared to the theoretical model of Blinowski-Rigaux employing the following model parameters,  $\gamma_0=2.9$  eV,  $\gamma_1=0.31$  eV,  $\delta=0.12$  eV, and  $E_f=-0.70$  eV. The band-structure model provided an adequate description of the experimentally determined data.

The charge-transfer coefficient per carbon atom  $f/l=0.012$  was determined from the observed sum of the dHvA frequencies. A determination of the fractional charge distribution for the stage-3 compound indicates

that there is a deficiency of charge in the internal graphite layer relative to the layers next to the intercalant.

The low frequency  $f_0$  is particularly interesting and is not explained completely at the present time. It may be evidence of the magnetic interferometer effect in which  $f_0$  is the interferometer orbit which combines with another frequency to form a series of combination frequencies.

#### ACKNOWLEDGMENTS

We appreciate the technical assistance provided by T. Olech. We wish to thank Dr. A.W. Moore for the HOPG graphite. The research was supported by the Natural Sciences and Engineering Research Council of Canada.

<sup>1</sup>E. Stumpf, *Mater. Sci. Eng.* **31**, 53 (1977).

<sup>2</sup>P. Behrens, V. Woebe, K. Jopp, and W. Metz, *Carbon* **26**, 641 (1988).

<sup>3</sup>W. R. Datars and P. K. Ummat, *J. Phys. Condens. Matter* **1**, 5031 (1989).

<sup>4</sup>J. Blinowski and C. Rigaux, *J. Phys. (Paris)* **41**, 667 (1980).

<sup>5</sup>I. M. Lifshitz and A. M. Kosevich, *Zh. Eksp. Teor. Fiz.* **29**, 730 (1956) [*Sov. Phys. JETP* **2**, 636 (1956)].

<sup>6</sup>M. S. Dresselhaus and G. Dresselhaus, *Adv. Phys.* **30**, 139 (1980).

<sup>7</sup>R. S. Markiewicz, *Phys. Rev. B* **28**, 6141 (1983).

<sup>8</sup>R. S. Markiewicz and C. Zahopoulos, *Phys. Rev. B* **27**, 7820 (1983).

<sup>9</sup>P. Behrens, H. Beuthien, H. P. Eickhoff, and W. Metz, *Synth. Met.* **23**, 95 (1988).

<sup>10</sup>A. Erbil, A. R. Kortan, R. J. Birgeneau, and M. S. Dresselhaus, *Phys. Rev. B* **28**, 6329 (1983).

<sup>11</sup>O. Takahashi, Y. Iye, and S. Tanuma, *Solid State Commun.* **37**, 803 (1981).

<sup>12</sup>G. Wang, H. Zaleski, P. K. Ummat, and W. R. Datars, *Phys. Rev. B* **37**, 9029 (1988).

<sup>13</sup>Y. Iye, O. Takahashi, and S. Tanuma, *Solid State Commun.* **33**, 1071 (1980).

<sup>14</sup>R. S. Markiewicz, H. R. Hart, L. V. Interrante, and J. S. Kasper, *Synth. Met.* **2**, 331 (1980).

<sup>15</sup>S. Tanuma, Y. Iye, O. Takahashi, and Y. Koike, *Synth. Met.* **2**, 341 (1980).

<sup>16</sup>G. Wang, P. K. Ummat, and W. R. Datars, *J. Phys. Condens. Matter* **3**, 787 (1991).